JOURNAL OF MATERIALS SCIENCE **38** (2003) 2771 – 2779

A comparative study of the MIG welding of Al/TiC composites using direct and indirect electric arc processes

R. GARCIA*, V. H. LOPEZ‡, E. BEDOLLA
Instituto de Investigaciones Metalúrgicas, UMSNH, PO Box 888, 58000, Morelia, Mich., México
E-mail: rgarcia@zeus.umich.mx

A. MANZANO
Centro de Investigación y de Estudios Avanzados, Instituto Politécnico Nacional, Fracc. Real de Juriquilla, CP 76230, Santiago de Querétaro, Querétaro, México

Metal inert gas welding of Al-1010/TiC/50p composites was carried out on 9 mm thick square bars by applying the electric arc directly and indirectly. Three pre-heating temperatures were used, 50, 100 and 150°C but only direct electric arc (DEA) was applied at room temperature. Welds were microstructurally examined and tested under tensile load. Complete penetration was achieved using both DEA and IEA methods. Uniform welds were obtained using indirect electric arc (IEA), meanwhile broadening was observed in the upper part in DEA welds facilitated by mixture of the base material with the filler. Microstructural observations showed good lateral fusion of the parent composites, little or no dissolution of TiC by IEA and only slight dissolution by DEA, which led to $TiAl_x$ formation during solidification. The presence of Al_4C_3 was not detected. Microhardness weld profiles revealed that the use of IEA reduces the heat affected zone (HAZ). Mechanical failure of the samples was consistently in the weld zone. Mechanical strength in IEA welds (182–186 MPa) was consistent irrespective of the pre-heating conditions and dependant only of the consumable (Al-2024). The mechanical strength of DEA welds was affected to some extent by the incorporation of the reinforcing particles into the weld region and wettability aspects inherent to the welding conditions. The use of IEA seems to be a suitable route for joining Al-based composites even when the reinforcement content is high.

1. Introduction

The interest in aluminum metal matrix composites (MMCs) reinforced with a variety of ceramics such as SiC and Al_2O_3 began 20 years ago. Nowadays the desirability of this class of materials is due to their improved and tailored specific mechanical and physical properties as well as wear resistance and electrical properties. However, the use of Al-based composites is still limited by their poor weldability when using conventional fusion welding processes [1, 2]. Exposure of the Al/SiC-type composite to temperatures above the liquidus of the aluminum alloys, as typically experienced in welding, results in a severe degradation of the mechanical properties caused by the formation of brittle and hygroscopic aluminum-carbon compounds [2, 3], mainly aluminum carbide. In addition, the conventional fusion welding processes produce a weld pool that has poor fluidity due to the presence of the ceramic phase and solidifies with a large volume of porosity in both the weld and HAZ because hydrogen evolves from the aluminum matrix, particularly, in MMCs manufactured by the powder metallurgy route. Ahearn *et al*. [1], found that vacuum degassing for long periods of time before welding reduced porosity in welds deposited by tungsten inert gas (TIG) welding and increased their mechanical strength, however the presence of Al_4C_3 was suspected. Altshuller and co-workers [4] reported that Al-6061/Al_2O_3 composites have a good degree of weldability with the metal inert gas (MIG) welding process and Stantz *et al*. [5] successfully welded Al-6061/B_4C/25p composites by both MIG and TIG processes. However, a number of researchers [2, 3, 6–8] have found that Al_4C_3 is always formed in welding Al-based composites reinforced with SiC, irrespective of the nature of the welding process employed, (i.e., TIG, MIG, capacitor discharge, laser or electron beam).

* Author to whom all correspondence should be addressed.
‡*Current address*: Advanced Materials Group, University of Nottingham, NG7 2RD, UK.

In previous work [9], the current authors have reported results obtained when welding aluminum sheets 12.5 mm thick by using the MIG welding process with an indirect electric arc (IEA). It was found that in virtue of the increase in the thermal efficiency of the novel process, complete penetration and uniform weld beads were obtained as well as; a reduction in the heat input to the workpiece and low percentage of dilution of the base material. The present study is an early step of a major project for welding MMCs, and it aims to assess the suitability of the novel MIG-IEA process to weld Al-based composites reinforced with a high ceramic content (∼50% TiC particles). Particular attention is focused on the configuration of the welds and their defects, dissolution of the reinforcement and on the mechanical efficiency of the joints.

2. Experimental details

2.1. Materials

The aluminum MMC was fabricated by means of a capillary infiltration technique [10–12]. TiC powder (∼1.23 μm mean particle size) was pressed uniaxially, without binder, to obtain green bars with 50% porosity. The green preforms were placed in a graphite crucible in contact with commercial purity aluminum (Al-1010) in a tube furnace and heated to 1100°C under a dynamic atmosphere of argon. The composites were machined to obtain square bars ∼9 × 9 × 65 mm. It should be highlighted that the majority of attempts to join MMCs by fusion welding have been carried out on thinner sections.

For welding, an ER4043 electrode, 1.2 mm in diameter, was employed. For the MIG welding process with IEA, small plates (∼25 × 5 × 200 mm) of 2024 aluminum alloy were used as feeding metal as illustrated in Fig. 1. The chemical compositions of the electrode ER4043, the aluminum employed to infiltrate the composites and the Al-2024 feed alloy are shown in Table I.

As a first trial, Al-2024 was chosen as a feeding material in the novel MIG-IEA process owing to its good fluidity in liquid state, good affinity for TiC in terms of wettability at elevated temperatures [12, 13] and finally because of its mechanical strength.

2.2. Welding procedure and parameters

The schematic drawing of the novel welding technique used in the present work is shown in Fig. 1. It consists of conventional fusion MIG welding process (where the droplets are spray transferred) with IEA and pure argon gas as a shield. The procedure has been described in detail elsewhere [9]. Prior to welding, the bars were cut through the mid-plane, across the width, and placed at a separation distance of 2–3 mm, then, butt-welding with direct current-reverse polarity was performed. The electric arc is then established between the solid electrode and an Al-2024 alloy in plate form (4–5 mm thick) placed over the parent composite. The resultant droplets, in the form of a spray, produce a molten pool on the plates and the liquid is fed at high temperature into the groove formed between the workpieces (Fig. 1a). The liquid metal melts the aluminum matrix in the composite, yielding the welded joint upon freezing (Fig. 1b).

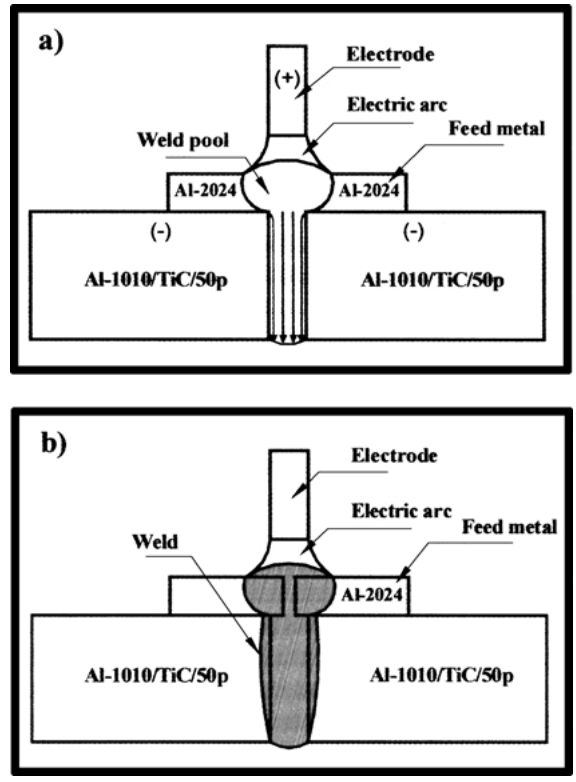

Figure 1 Schematic drawing of the MIG welding process with IEA: (a) flux of molten metal into the joint and (b) profile of the weld upon freezing.

The welding conditions of the DEA and IEA techniques employed in the present work are shown in Table II. Preliminary trials showed that in order to achieve full penetration and good lateral fusion on the base composites in one welding pass, it was necessary to pre-heat the joints before welding. For this reason and aiming to asses any benefit of increasing this parameter, three pre-heating temperatures were used, namely; 50°C, 100°C and 150°C. To accomplish welding at room temperature, two welding passes were deposited using the conventional MIG process (DEA), one either side of the square edge butt-weld joint.

TABLE I Chemical composition of the metallic materials employed (%wt)

Material	(%)Al	(%)Si	(%)Fe	(%)Cu	(%)Mn	(%)Mg	(%)Cr	(%)Ni	(%)Zn	(%)Ti
ER4043	93.3	5.25	0.8	0.3	0.05	0.05	—	—	0.10	0.02
Al-1010	99.1	0.2	0.65	0.005	0.002	0.014	0.012	0.009	0.002	—
Al-2024	91.8	0.35	0.36	4.46	1.08	1.86	0.017	—	0.047	—

TABLE II MIG welding parameters used to join Al-1010/TiC/50p composite bars using DEA and IEA processes

Parameter	Value
Current	250 A
Voltage	22 v
Travel speed	3.6 mm s^{-1}
Argon flow rate	22 1 min^{-1}
Pre-heating temperature 25, 50, 100 and 150°C	
Heat input	5.5 kJ s^{-1}
Stick out	12 mm

2.3. Welds examination and mechanical testing

In order to disclose the microstructure in the weld profile, the HAZ and unaffected parent composite, standard metallographic techniques were used to prepare the samples but the use of water was omitted. Microstructural characterisation was performed by means of optical microscopy and scanning electron microscopy (SEM) attached to an energy dispersive X-ray spectroscopy (EDX) system. X-ray diffraction was used to identify the phases present in the welds by using Cu K_α radiation for 2θ values between 10–90° with a scanning step of 0.02°. Transverse hardness weld profiles were generated by applying a 50 grams load with a Vickers indent. Indentation lines were carried out at approximately $^3/_4$ of the weld height on mirror-like polished samples. Tensile tests were carried out, at room temperature, on a universal testing machine at a cross head speed of 0.083 mm s^{-1}. The mean value of at least three samples is reported.

3. Results and discussion

3.1. Geometry of the welds

Typical cross section profiles of the welds obtained by means of DEA and IEA are compared in Fig. 2. The arrows indicate the widths of the welds in the top of the parent composites. In both cases the operative parameters for the process are listed in Table II. Regarding the DEA welds, from Fig. 2a and b, it can be observed that complete penetration and broadening of the beads occurs at the top of the workpieces (W regions), which were initially square. The distortion of the composite is greater with pre-heating at 100°C than at 150°C. Macroscopic observations indicate that at low pre-heating temperatures the composites are more severely affected by the thermal cycle imposed upon them. The critical case is presented when the welds are deposited at room temperature, so that incomplete penetration is obtained and a second welding pass on the counterpart is required. The presence of macroporosity in the sample preheated at 100°C and the convex shape of the overlap of the weld, compared to at 150°C null macroscopic porosity and a concave shape suggests a poorer fluidity for the molten pool in the former case.

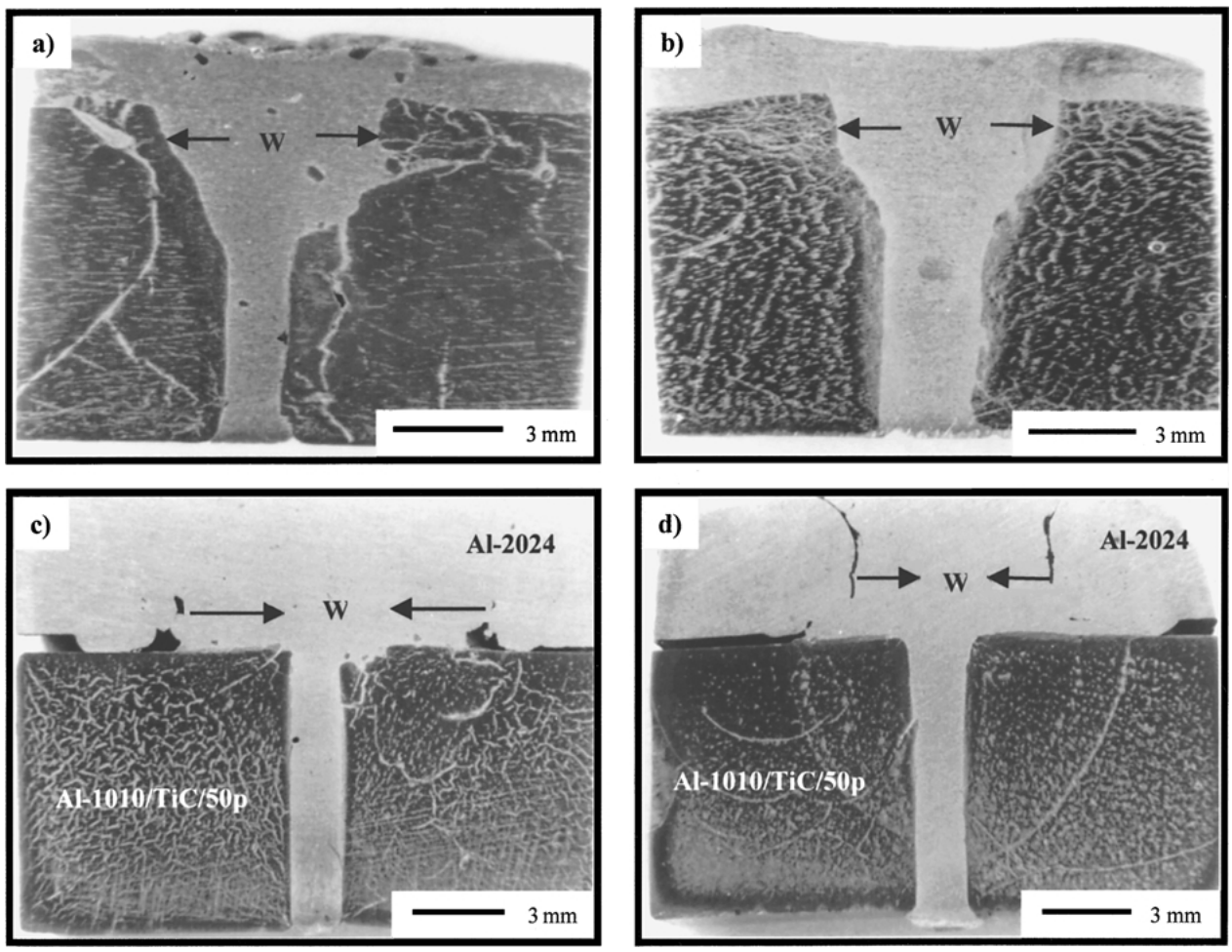

Figure 2 Profiles of the welds deposited by: (a) DEA at 100°C, (b) DEA at 150°C, (c) IEA at 100°C, and (d) IEA at 150°C.

Regardless of the pre-heating temperature employed, a broad weld bead on the top was always exhibited when applying the electric arc in a direct manner, which is explained due to the powerful electric arc projected on the base composite material, the high temperature reached in those zones and the turbulent stream created in the molten pool. For this reason, melting and mixing between the filler and the parent composite is expected.

On the other hand, in welds deposited by IEA (Fig. 2c and d), the distortion suffered by the parent composite is minimum. Hence, uniform profiles are obtained. Very little macroporosity was observed at any of the pre-heating temperatures. It was demonstrated in a previous work [9], that the use of IEA improves the thermal efficiency of the MIG process and reduces the extent of base material melted. Furthermore, it was found that increasing the pre-heating temperature increases the thermal efficiency of the process. Thus, macroscopic characteristics indicated above are expected to occur during welding of Al-based composites by IEA.

3.2. Microstructure and reaction products

Independently of the method employed, continuity of the aluminum composite matrix with the aluminum filler of the weld was achieved, as can be appreciated in Fig. 3. However, microstructural differences in the welds obtained by both techniques are evident. The microstructure between the HAZ and the weld in a sample welded using DEA is shown in Fig. 3a and b. It can be clearly observed that TiC particles had been transferred from the composite to the weld, meaning that mixture of filler and base material occurred. Particulate segregation delineates the grain boundaries in the weld and small regions with TiC particles uniformly distributed are also observed. Microporosity and needle-like intermetallics can be distinguished, which were found to be Ti-Al compounds according to EDX results, as shown in Fig. 4. In Fig. 3a the significant extent of matrix fusion on the parent composite caused by the heat input by the electric arc and the spray transfer mechanism can be observed. Fig. 3c and d show the weld interface produced by IEA, no HAZ can be clearly identified, on the contrary, a discrete uniform weld/composite interface is observed and the degree of aluminum matrix melting is minimum as is the transfer of TiC particles into the weld. The violent action of the electric arc and the turbulent molten pool occur on the feeding plates, thus, the abscence of TiC particulates in the weld and the degree of fusion in the parent composites are explained. According to the EDX analysis, the majority of the grain boundary precipitates observed in Fig. 3c correspond to $CuAl_2$ and $MgCuAl_2$.

In order to emphasize the superheating suffered by the parent composite, as a result of the direct application of the electric arc, it should be mentioned that clusters of TiC particles which were partially sintered,

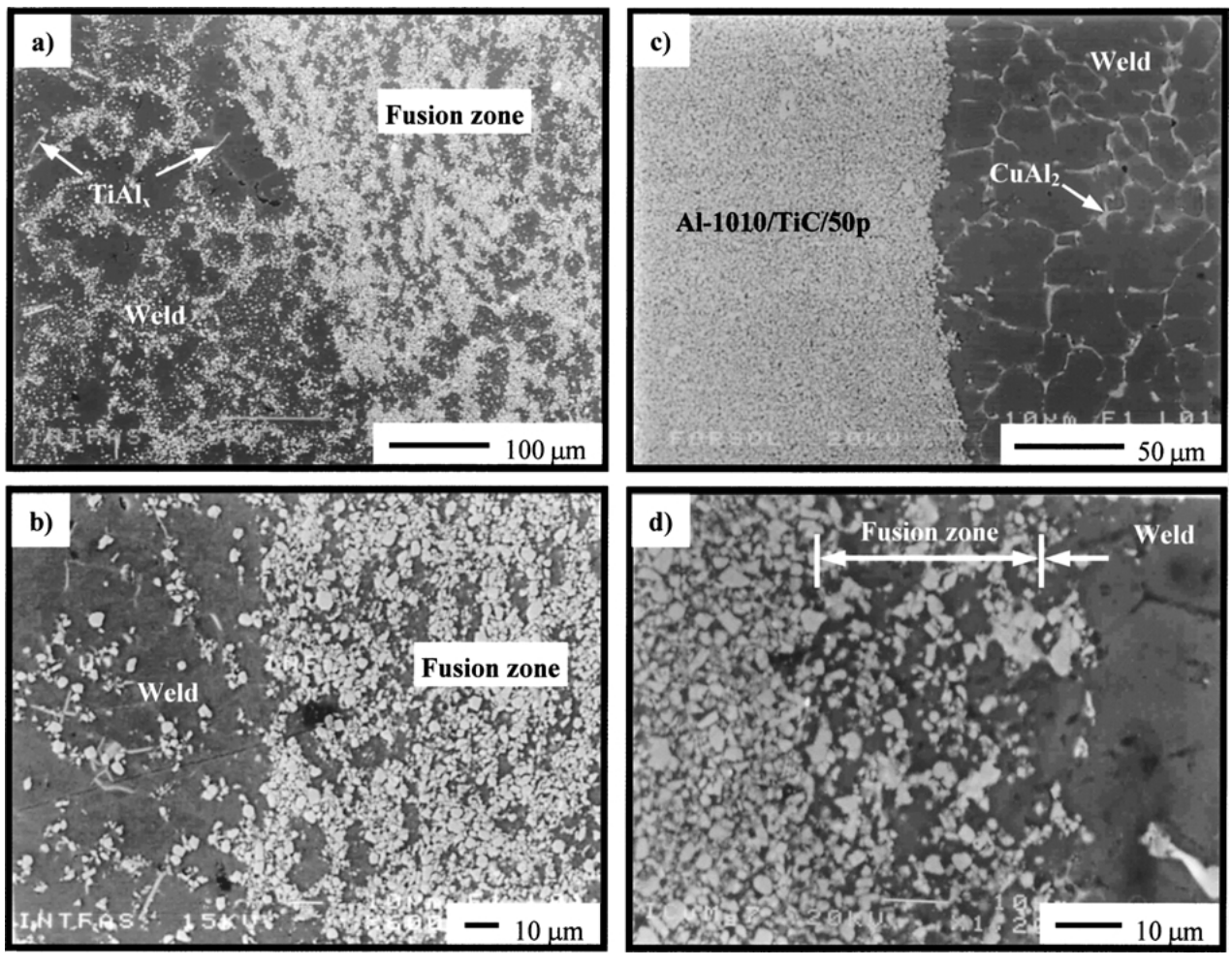

Figure 3 Microstructure of the welds preheated at 150°C and produced by: (a) and (b) DEA, and (c) and (d) IEA.

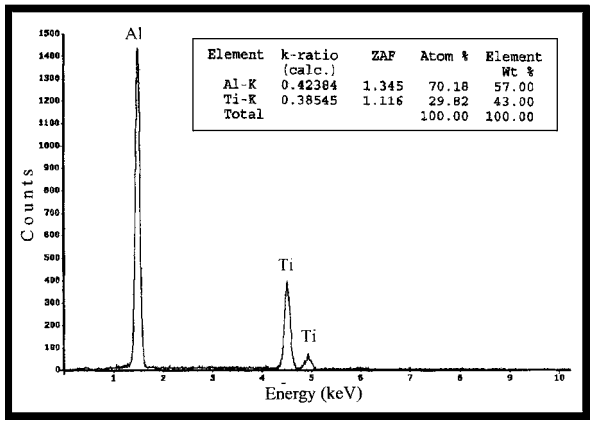

Figure 4 Typical EDX analysis of the needle-like intermetallics found in DEA welds.

were found in some regions near to the top of the weld. The presence of titanium aluminides indicates that dissolution of TiC occurred. These features are shown in detail in Fig. 5. It is also observed that TiC particles are present along with eutectic Si from the 4043 filler alloy in the inter-dendritic regions. It was also found that silicon is incorporated in some titanium aluminides, as shown in the EDX analysis in Fig. 5.

Although the SEM examination of the welds showed dissolution of the TiC, evidence of Al_4C_3 formation was not detected and XRD studies performed in the welds under the different experimental conditions corroborated the SEM observations. Fig. 6 shows the

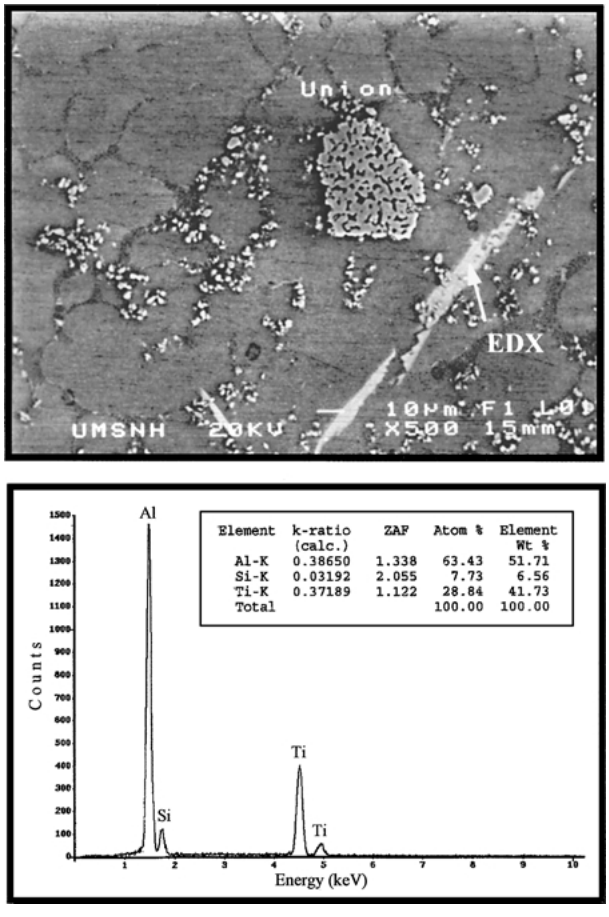

Figure 5 Detail of the HAZ in a weld obtained by DEA at 150°C and EDX analysis of the acicular phase.

x-ray difractograms of samples welded by both methods in the different pre-heating conditions. Further to titanium aluminides being observed and identified previously through SEM and EDX analysis, respectively, a complex Ti-Al-C compound was identified mainly in DEA welds. In IEA specimens, the $CuAl_2$ compound was nearly in the limit of detection so that it was hardly distinguished in the XRD difractograms. Traces of aluminum oxide are observed in IEA welds by XRD. It seems that extreme oxidation occurred in the Al-2024 plates during pre-heating, in such a way that, the break up effectiveness of the operation mode (direct current-reverse polarity) was insufficient to dissociate the oxide film, giving rise to insoluble Al_2O_3 dross trapped within the weld metal. This is an undesirable effect since drosses act as inclusions which decrease the mechanical strength of the weld. It is worth to say that welds were again X-ray analysed after removing the Al-2024 plates and it was found that the Al_2O_3 traces disappeared. This fact does not necessarily mean that the welds were drosses free, but it might suggests that their concentration was mostly on the plates region.

Notwithstanding that bulk formation of new phases was not detected, the broadening of some peaks along with changes in the relative intensity and shape of the peaks, might suggest that some interactions occurred in the variety of samples. However, overlapping and the very low intensity of the peaks, make it difficult to ascertain the identification of additional compounds using this technique. Special attention was however paid to looking for the main peaks of Al_4C_3 and according to the joint committee for powder diffraction file (JCPDF) files no matching was found.

In metal/ceramic systems, the formation of new phases and their extent depends on the starting materials, the processing route and of course additional heat treatments. In particular, and in spite of Al_4C_3 was found in wetting studies performed by the sessile drop method [13], when manufacturing Al-based composites reinforced with TiC by the infiltration technique, in the temperature interval of 900–1200°C, no bulk reaction has been observed [10–12], and only trace levels of Ti_3AlC has been detected through XRD analysis [12]. However, there are disputes about the stability of Al_4C_3 in the Al-Ti-C system [14–21]. Banerji and Reif [14] argued that TiC is unstable in molten Al below 1177°C meanwhile Fine and Conley [15] claimed that TiC is thermodynamically more stable than Al_4C_3 and Rapp and Zheng [16] concluded that during normal grain refining operations, TiC is more stable than Al_4C_3, but also, that when Ti is dissolved in molten Al below 0.5% wt, Al_4C_3 is more stable than TiC in the interval between 877–1527°C. On the other hand, a number of authors suggest that the stability transition in the Al/TiC system is between 800 to 890°C and that TiC is stable above this temperature [17–21], according to the reversible reaction;

$$3TiC + 13Al(l) \Leftrightarrow Al_4C_3 + 3TiAl_3 \qquad (1)$$

Nevetheless, Al_4C_3 formation in the Al/TiC system seems to be controlled by relatively slow kinetics rather

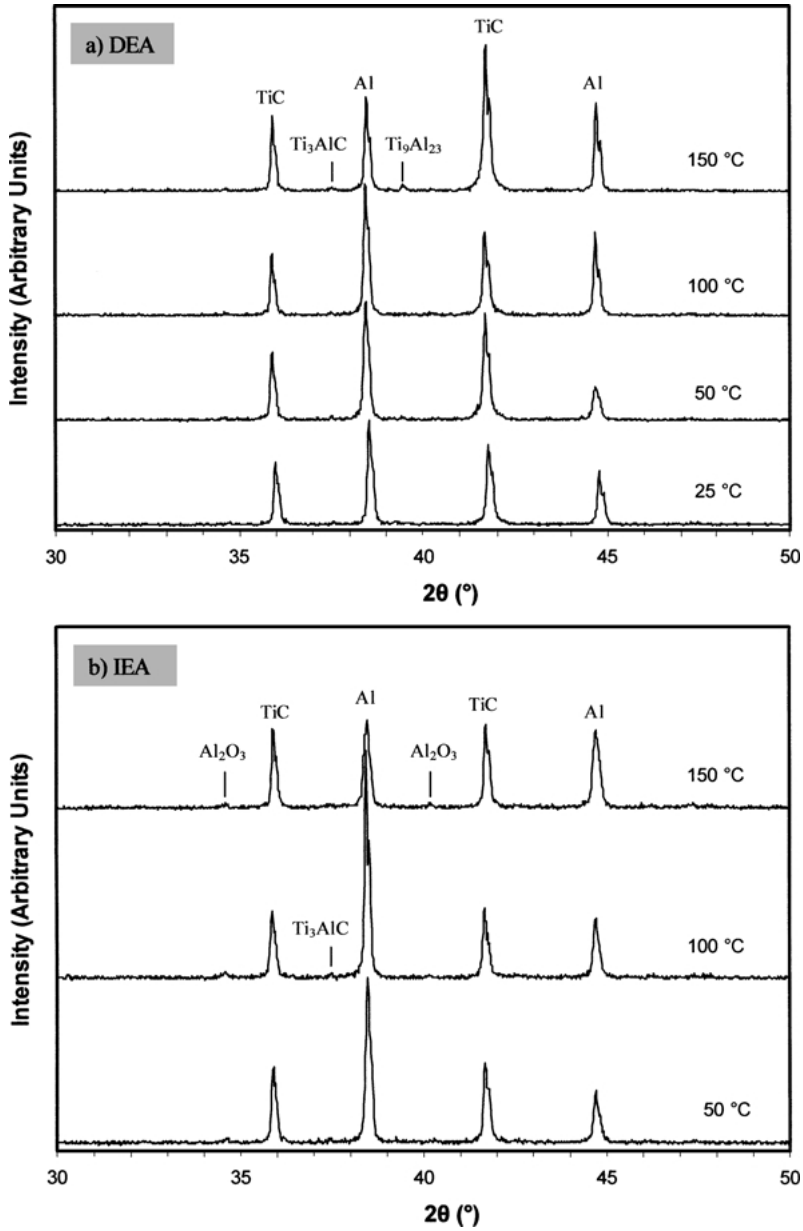

Figure 6 XRD patterns of the welds obtained at the different pre-heating temperatures: (a) DEA and (b) IEA.

than by thermodynamics, since it only appears after long exposures to heat treating [18, 21–24]. Arc fusion welding is a relatively fast melting/freezing process, so the non-appearance of Al_4C_3 is expected and the precipitation of acicular $TiAl_x$ intermetallics during cooling and solidification may be expected due to the dissolution of TiC in the high temperature regions of the weld pool. Current research is being carried out to model the distribution of temperatures in the weld profile during welding. Traces of the P-phase were also detected mainly in IEA welds obtained in this study (Fig. 6) and it is thought that it formed also due to the dissolution of TiC during welding, since it was not detected in the parent composites before welding. The mechanism of the formation of Ti_3AlC is even more uncertain. Banerji and Reif [14] found this compound when processing below 1000°C. Mohanty and Gruzleski [25] reported complete decomposition of TiC in an Al-7%Si alloy forming Al-Ti-Si compounds of the type found in DEA welds (Fig. 5) and also the complex carbide Ti_3AlC. In the MIG-DEA process the electric arc is established directly on the Al/TiC composite, meanwhile in the MIG-IEA process it occurs in the Al-2024 plates, meaning that the high silicon filler, ER4043, is prone to interact with the parent composite in the former case. The interval of stability in the Al/TiC system in presence of Si is not established. Thus, two aspects may be account for the presence of the P-phase in DEA welds; the wide interval of temperatures developed in the process, and the high silicon content in the filler. Elucidating about these matters goes beyond the scope of the present work, but it is important to remark that, at least by means of the characterisation techniques employed, Al_4C_3 was not detected.

3.3. Mechanical properties and fracture

Fig. 7 shows transverse microhardness profiles carried out on welds deposited at pre-heating temperatures of 100 and 150°C by DEA and IEA processes. Generally speaking, comparison between DEA and IEA hardness profiles shows that DEA welds are wider than IEA

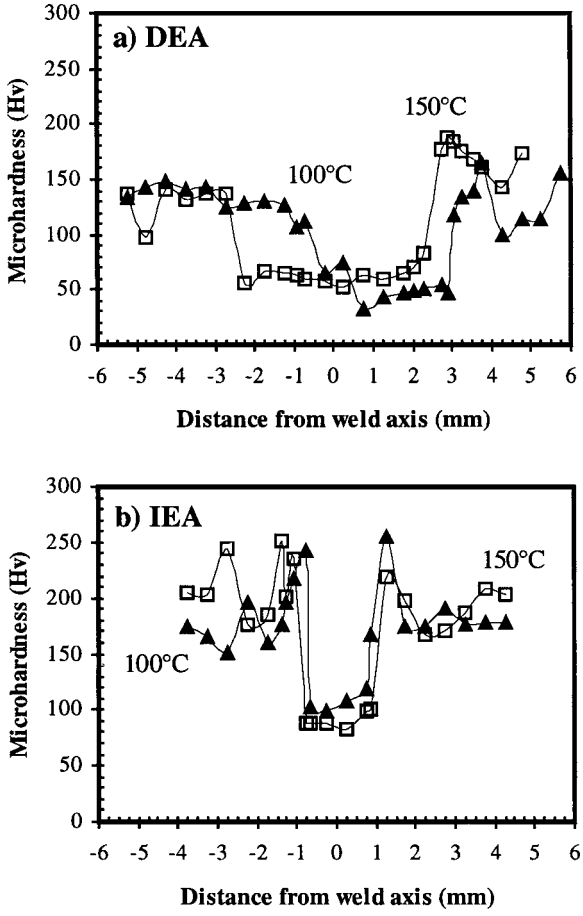

Figure 7 Transverse microhardness weld profiles of (a) DEA and (b) IEA welds pre-heated at 100 and 150°C.

welds, according to weld beads observed in Fig. 2. It is also noticeable that average hardness values, within the weld are lower for DEA welds. This fact is in direct relation with the chemical composition of the welds. Whilst DEA welds comprise of an Al-4.5 wt% Si filler alloy, IEA welds are a mixture of Al-4.5 wt% Si and Al-2024 filler alloys.

Average DEA hardness values are slightly lower than those measured in IEA welds in the base metal. This difference confirms that the direct application of the electric arc on the base composite leads to a greater thermal affection, being reflected in the distortion suffered on the workpieces, redistribution of reinforcement in the HAZ, as observed in Fig. 3a and b, and therefore in lower hardness. The non-symmetrical hardness profiles, in Fig. 7a for DEA welds, support these observations. On the other hand, IEA hardness profiles are rather symmetric, as a result of the uniformity achieved in the weld beads and the limited redistribution of reinforcement in the fusion zone. Maximum peak hardness values measured next to the weld metal/base composite interface suggest that a little HAZ exists. Diffusion of intermetallic phases to these regions might accounts for these high values. Maximum or minima peak hardness values beyond these regions, are likely to be due to the wide particle size distribution (0.03 to 5 μm) of the TiC powder use to fabricate the composite, which can lead to significant variations in hardness.

Tensile tests results are shown in Table III. With respect to IEA welds, it can be seen that no benefit is

TABLE III Ultimate tensile strength of the welded joints (MPa)

Pre-heating temperature	25°C	50°C	100°C	150°C
DEA welds	214	181.12	183.43	204.56
IEA welds	—	183.33	181.79	185.96

Al-1010/TiC/50p (219.73 MPa), Al-2024-O (186 MPa), ER4043 (200 MPa).

obtained by increasing pre-heating temperatures, instead, the strength appears to be in relation to the tensile strength of the Al-2024 feed alloy in the as cast condition. The same situation is likely for DEA welds preheated at 50 and 100°C, it means, the mechanical response is related to the ER4043 filler and the defects generated during the welding and solidification events. Mechanical efficiency of the welds was calculated with respect to the mechanical strength of the base composite tested at room temperature (Al-1010/TiC/50p = 219.73 Mpa). An average of 83.5% mechanical efficiency is calculated for joints welded by IEA as shown in Table IV. The use of pre-heating, prior welding, provides a slower rate of cooling, as a result, shrinkage stresses and gas entrapment are reduced, which in turn should lead to an enhancement of the mechanical properties. However, this response is not manifested in the tensile strength of IEA welds. The presence of Al_2O_3 dross in the welds, as a result of the oxidation of the Al-2024 plates during pre-heating, might explain, in part, this behavior.

Three cases can be distinguished for DEA welds; (1) room temperature, (2) 50 and 100°C, this case was mentioned above, and (3) 150°C. In spite of the fact that at room temperature one welding pass in each side was needed, these welds exhibited the highest ultimate tensile strength. According to the examination of the welds, a significant dispersion of TiC particles in the weld occured due to the double welding pass, so that reinforcing and refining actions are anticipated [14, 26], increasing the tensile strength and as a consequence the mechanical efficiency of these joints. The third case is at the highest pre-heating temperature, 150°C. Under this condition and in comparison with the values calculated for specimens preheated at 50 and 100°C, a 10% increase of the efficiency of these joints was measured. The improvement is likely the response to an increase in the thermal efficiency of the process, giving rise to less pronounced defects during freezing (trapped gas and shrinkage pores) and enhanced wetting properties of the particles transferred into the molten pool.

Fig. 8 shows the fracture surfaces of welds obtained at room temperature (Fig. 8a) and preheated at 150°C (Fig. 8b and c). In general, no noticeable differences were observed between DEA and IEA samples. Fractures consisted of shallow dimples and few equiaxial dimples of different sizes, trans-granular breakage

TABLE IV Mechanical efficiencies of the welded joints (%)

Pre-heating temperature	25°C	50°C	100°C	150°C
DEA welds	97.4	82.4	83.4	93.0
IEA welds	—	83.4	82.7	84.6

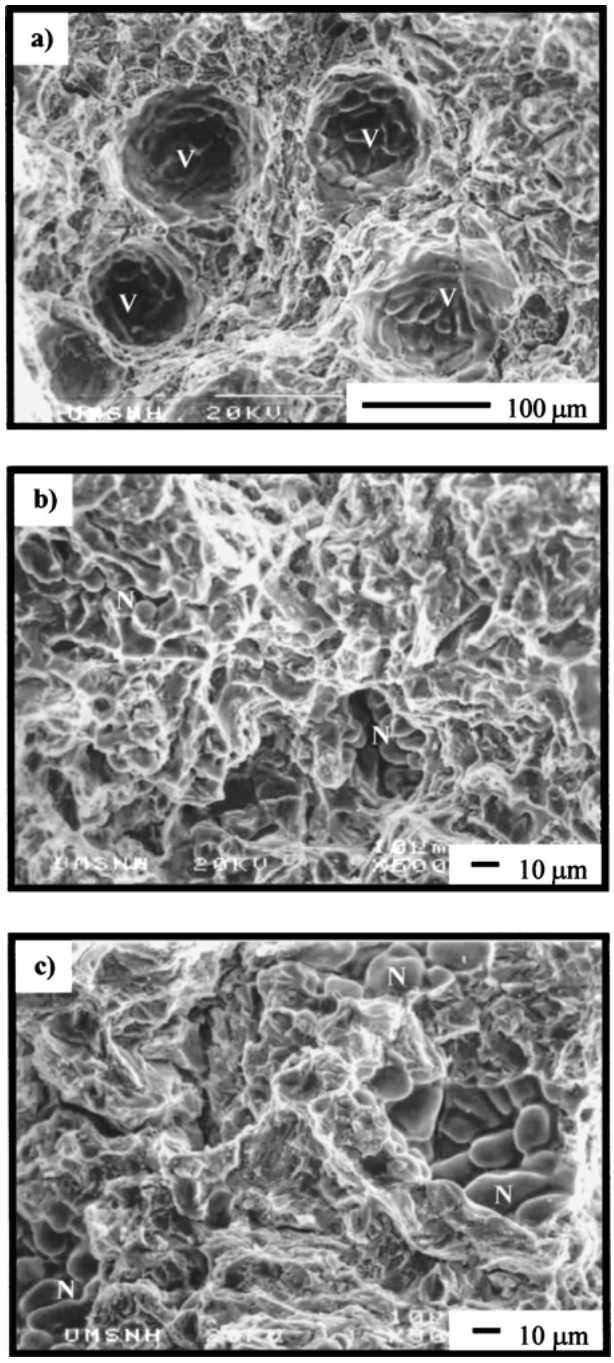

Figure 8 Fracture surfaces of tensile specimens: (a) DEA at room temperature, (b) DEA at 150°C, and (c) IEA at 150°C.

and brittle inter-granular decohesion were observed. Shrinkage and trapped gas porosity are likely to have dictated the fracture path. These features along with the shape of the stress-strain curves, which are not shown, evidence the poor ductility of the welds, which might be ascribed to the small volume of ductile weld metal. Susceptibility to gas entrapment is greater at low pre-heating temperatures, because of that, samples welded at room temperature and 50°C, exhibited relatively small rounded cavities (V), as observed in Fig. 8a, which resemble coalescence of smaller gas bubbles. The occurrence of gas porosities was noticeably decreased in samples preheated at 150°C and shrinkage pores with dendrite nodules (N) were mainly found (Fig. 8b and c) having larger pores in IEA welds at 150°C, which reduced the ultimate tensile strength of the weld, as shown in Table II. The fact that the failure occurred in the weld, is an indication of the good bonding achieved at the weld/composite interface, irrespective of the method or pre-heating condition employed. The good affinity between TiC and liquid Al in terms of wettability is well documented at high temperature [10, 12, 13], meaning that TiC preforms can be pressureless infiltrated by Al and its alloys [10–12]. Furthermore, it has been reported that in the MIG welding process, the drops in the spray transfer mode are detached at high temperatures, around 2200°C, using the ER 4043 electrode [27, 28]. Thus, although wetting is a time and temperature dependant phenomenon, spontaneous wetting of molten Al on TiC is expected during welding in virtue of the high temperature at which the liquid aluminum is supplied into the joint.

4. Conclusions

Welding of Al-based composites reinforced with a high ceramic content of TiC particles was possible by the MIG process using both DEA and IEA techniques. Complete penetration was achieved in one welding pass by pre-heating the parent composite above 50°C but a double welding pass was needed to weld the composite by DEA at room temperature. Whilst areas free of dispersed particles and uniform welds are obtained by IEA, wide weld beads in the arc applied region with some incorporation of the reinforcing particles, are produced by DEA. Negligible dissolution of TiC occurs by using IEA and although some occurred by DEA, the deleterious aluminum carbide compound was not detected.

Evaluation of the mechanical efficiency in the welds indicates that, independently of the welding technique and pre-heating condition employed, TiC-reinforced aluminum MMCs exhibited a good degree of weldability by the MIG process. Although the efficiencies exhibited by IEA are lower than by DEA, the former looks attractive due to the weld profiles that can be obtained with a reduced HAZ. In addition, it is thought that the mechanical strength might be enhanced by using composite with low reinforcement content as a feeding material. Thus, the use of the MIG welding process with IEA can be considered an alternative for solving some problems encountered in welding of MMCs.

Acknowledgements

The authors wish to thank to Escuela de Ingeniería Mecánica of the UMSNH for making available their facilities. The helpful comments about the manuscript by A. R. Kennedy are indebted. Financial support from Coordinación de la Investigación Científica of the UMSNH is also acknowledged.

References

1. J. S. AHEARN, C. COOK and S. G. FISHMAN, *Metal Constr.* **14** (1982) 192.
2. M. B. D. ELLIS, M. F. GITTOS and P. L. THREADGILL, *Mater. World* **2** (1995) 415.
3. A. URENA, M. D. ESCALERA and L. GIL, *Compos. Sci. Technol.* **60** (2000) 613.

4. B. ALTSHULLER, W. CHRISTY and B. WISKEL, in Proceedings of the 2nd International Conference on Trends in Welding Research, May 1989, edited by S. A. David and J. M. Vitek (ASM, Metals Park, OH, 1990) p. 305.
5. T. M. STANTZ, D. K. AIDUN, D. J. MORRISON, T. DIEBOLD, P. MARTIN and M. BRISKOTTER, in Proceedings of the 3rd International Conference on Trends in Welding Research, June 1992, edited by S. A. David and J. M. Vitek (ASM Materials Park, OH, 1993) p. 781.
6. C. D. LUNDIN, J. C. DANKO and C. J. SWINDEMAN, in Proceedings of the 2nd International Conference on Trends in Welding Research, May 1989, edited by S.A. David and J.M. Vitek (ASM Materials Park, OH, 1990) p. 303.
7. T. J. LIENERT, E. D. BRANDON and J. C. LIPOLD, *Scripta Metall. Mater.* **28** (1993) 1341.
8. J. H. DEVLETIAN, *Weld. J.* **66** (1987) 33.
9. R. GARCIA, "Union de matriales compuestos del tipo Al(1010)/TiC(51%) por medio del proceso de soldadura MIG con arco electrico indirecto," PhD theses, Universidad Autonoma de Queretaro, Mexico, 2002.
10. D. MUSCAT and R. A. L. DREW, *Metall. Mater. Trans.* A **25** (1994) 2357.
11. A. ALBITER, C. A. LEON, R. A. L. DREW and E. BEDOLLA, *Mater. Sci. Eng.* A **289** (2000) 109.
12. A. CONTRERAS, V. H. LOPEZ, C. A. LEON, R. A. L. DREW and E. BEDOLLA, *Adv. Technol. Mater. & Mater. Process. J.* **3** (2001) 27.
13. V. H. LOPEZ, C. A. LEON, R. A. L. DREW and E. BEDOLLA, *J. Mater. Sci.* **37** (2002) 3509.
14. A. BANERJI and W. REIF, *Metall. Trans.* **17** (1986) 2127.
15. M. E. FINE and J. G. CONLEY, A *ibid.* **21** (1990) 2609.
16. R. RAPP and X. ZHENG, *ibid.* **22** (1991) 3071.
17. J. C. SCHUSTER, H. NOWOTNY and C. VACCARO, *J. Solid State Chem.* **32** (1980) 213.
18. J. C. VIALA, C. VINCENT, H. VINCENT and J. BOUIX, *Mater. Res. Bull.* **25** (1990) 457.
19. L. SVENDSEN and A. JARFORS, *Mater. Sci. and Technol.* **9** (1993) 948.
20. A. R. KENNEDY, D. P. WESTON, M. I. JONES and C. ENEL, *Scripta Mater.* **42** (2000) 1187.
21. A. R. KENNEDY, D. P. WESTON and M. I. JONES, *Mater. Sci. Eng.* A **316** (2001) 32.
22. K. SATYAPRASAD, Y. R. MAHAJAN and V. V. BHANUPRASAD, *Scripta Metall. Mater.* **26** (1992) 711.
23. A. B. PANDEY, R. S. MISHRA and Y. R. MAHAJAN, *Mater. Sci. Eng.* A **206** (1996) 270.
24. R. MITRA, M. E. FINE and J. R. WEERTMAN, *J. Mater. Res.* **8** (1993) 2370.
25. P. S. MOHANTY and J. E. GRUZLESKI, *Scripta Metall. Mater.* **31** (1994) 179.
26. A. E. KARANTZALIS and A. R. KENNEDY, *Mater. Sci. Forum* **217–222** (1996) 253.
27. M. J. LU and S. KOU, *Weld. J.* **68** (1989) 382s.
28. *Idem.*, *ibid.* **68** (1989) 452s.

Received 21 August 2001
and accepted 3 April 2003